A Preliminary Assessment of Projected CMIP6 Extreme Rainfall in the Subarnarekha River Basin

Santosh Kumar
Department of Civil Engineering, National Institute of Technology Patna, Patna, Bihar 800005, India
santoshk.phd19.ce@nitp.ac.in (corresponding author)

Vivekanand Singh
Department of Civil Engineering, National Institute of Technology Patna, Patna, Bihar 800005, India
vsingh@nitp.ac.in

Received: 30 June 2025 | Revised: 11 July 2025 | Accepted: 16 July 2025

 DOI: https://doi.org/10.48084/etasr.13075

ABSTRACT

This study aims to evaluate the effectiveness of Coupled Model Intercomparison Project Phase 6 (CMIP6) climate models in predicting the rainfall patterns by comparing the model outputs to the observed rainfall data (2015-2023) acquired from the India Meteorological Department (IMD) in Subarnarekha river basin in India. The analysis methods include statistical tools, such as Correlation Coefficients (CC), Root Mean Square Error (RMSE), Sen's slope estimator, Mann–Kendall (MK) trend test, and monthly Taylor diagrams. The accuracy and reliability of the CMIP6 models have been assessed systematically for different regions, namely Ranchi, Jamshedpur, and Digha. Two simulation models of CMIP6 are used: BCC-CSM2-MR (BCC) and CanESM5 (Can). The BCC model suggests a stronger correlation with the observed data in comparison to the Can model, thus suggesting their robustness in capturing the regional rainfall patterns. BCC offered an average CC of 0.4 with an average standard deviation between 30% and 40% in all the three regions. Conversely, the Can model presented substantial discrepancies, particularly in terms of standard deviation, indicating areas for model improvement. Furthermore, trend analysis is performed on the observed and predicted rainfall data. The results suggested not statistically significant decreasing trends in all regions except during monsoon seasons and especially in June. These findings underscore the importance of model selection in climate impact studies and highlight the need for ongoing refinement of the climate models to enhance the predictive accuracy.

Keywords-Cmip6; extreme rainfall; rain simulations; bias; subarnarekha river basin

I. INTRODUCTION

Temperature and precipitation are two of the most common meteorological parameters utilized to study the impact of climate change, which can lead to water scarcity. Consequently, the reduced water accessibility impacts sectors, such as agriculture, and further escalates severe weather patterns, like floods, droughts, and heatwaves [1]. It is essential to forecast these climatic variables to reliably respond to these challenges and plan resilient infrastructure. Global Climate Models (GCMs) and Regional Climate Models (RCMs) are two of the models that provide such simulations, which can integrate historic records with key variables, such as surface temperature and precipitation [2, 3].

The use of GCMs at regional scales is limited by a number of uncertainties, including coarse resolution, inaccurate aerosol parameterization, unstable boundary conditions, greenhouse gas trails, and model biases [4, 5]. Moving from global to local scales introduces additional uncertainties caused by the internal climate variability, human impact, and the inherent difficulty of physical modeling [6]. Therefore, a careful examination of the existing models must be performed before selecting the most appropriate GCM to analyze the regional impacts of temperature and precipitation.

World Climate Research Program (WCRP) provides a coordinated scheme of the global climate modeling, the Coupled Model Intercomparison Project (CMIP). The CMIP backs up historical validation and projection research of various models [7]. The sixth generation of CMIP (CMIP6) includes more than 50 modeling centers, enhanced physical parameterizations, higher spatial resolutions, and an enhanced carbon-nitrogen cycling [8]. Authors in [9] employed the CMIP5 and CMIP6 models to test the performance utilizing RMSE, CC, and Skill Score (SS).

Statistical or dynamical downscaling can correct the biases from the GCM outputs. The statistical techniques provide empirical links between the output of the models and the

observed data, whereas dynamical techniques combine RCMs with GCMs to perform high-resolution simulations [10, 11]. Statistical downscaling tends to be computationally and economically efficient due to the lower computational and storage requirements. In contrast, dynamic methodologies offer a more accurate representation of physical processes but they require greater computational resources and storage [12].

CMIP6 projections under Shared Socioeconomic Pathways (SSPs) are widely used in hydrological research. SSPs refer to potential future scenarios describing the future trends in global society, demographics, and economics to explore the impacts of the climate change and related policies. SSP1-2.6 and SSP2-4.5 represent low to moderate emission scenarios, while SSP3-7.0 and SSP5-8.5 indicate high-emission future scenarios with greater socioeconomical risks. In the Subarnarekha River Basin, bias-corrected CMIP6 data were rescaled to local rain-gauge data using 0.25° linear interpolation [13]. Understanding these projections is crucial to the evaluation of hydrological responses and to develop effective strategies to manage the impact of climate change in vulnerable basins, like Subarnarekha [3-14].

Subarnarekha River in situated in Jharkhand state, Eastern India and the main water resource is rainfall [15]. Therefore, it is necessary to manage the water resources for sustainable agriculture and additionally mitigate the effect from natural disasters, such as floods and droughts. Authors in [16] analyzed the impact of the climate change in the hydrological parameters of the basin in the present climate change scenario. The results indicated extreme shortage of water and extreme natural hazards. The accuracy of historical and future simulations has yet to be verified in GCMs and RCMs prior to their application in computing the current and projected climate change, especially regarding extreme hydrological events.

II. STUDY AREA AND DATA

The Subarnarekha River basin, illustrated in Figure 1, flows through Jharkhand in West Bengal and through Orissa in Eastern India, and is considered the smallest of the country's 14 major river basins. The Subarnarekha River has a total catchment area of 19,296 km² [15]. The catchment area's state-wise distribution is as follows: Jharkhand accounts for the larger proportion of the area (68.4%), followed by West Bengal (15.5%) and Orissa (16.1%). The main weather event affecting the river basin is the south-west monsoon, which starts in June and ends in October.

The Subarnarekha River is a peninsular river and primarily dependent on rainfall. The river basin experiences scorching summers and mild winters due to its tropical environment. The average yearly rainfall of the basin is 1800 mm, and its average monthly temperature varies from 9.0 °C in December to 40.5 °C in May. The yearly average maximum and minimum temperatures are 32.4 °C and 18.0 °C, respectively. An increase is observed in the frequency of extreme weather events and drastic weather shifts, leading to a decrease in the available surface and ground water.

Daily observed rainfall data from 2015 to 2023 are utilized in this study, acquired by rain gauge stations located at Ranchi, Jamshedpur, and Digha regions and are operated by IMD. Extreme monthly values are extracted and by employing the Thiessen polygon method the area distributions for each rain gauge station is determined and presented in Table I.

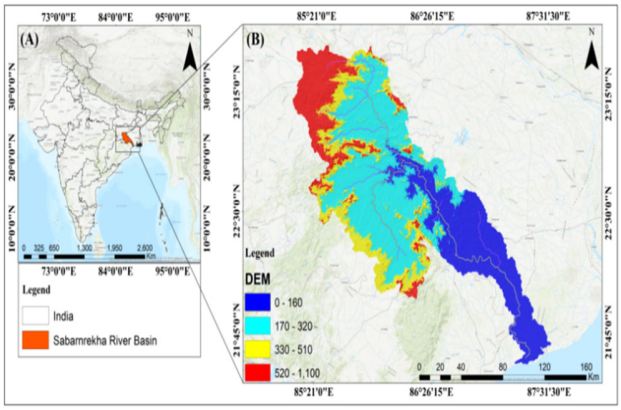

Fig. 1. Subarnarekha River basin and under-study region.

TABLE I. RAIN GAUGE STATION DETAILS

Station name	Area (km²)	Altitude (m)	Latitude (N)	Longitude (E)
Ranchi	2278.55	651	23° 20' 39"	85° 17' 46"
Jamshedpur	4769.00	135	22° 48' 20"	86° 12' 11"
Digha	12327.97	6	21° 38′ 18″	87° 30′ 35″

The study area is divided into three regions, namely Upper (Ranchi), Middle (Jamshedpur), and Lower (Digha). This study also utilizes monthly rainfall data from SSPs simulations from CMIP6 models that are part of the Intergovernmental Panel on Climate Change (IPCC) Sixth Assessment Report (AR6) under various scenarios [8, 17]. The details of two selected CMIP6 simulation models with different scenarios are listed in Table II. In both models the following scenarios are chosen: SSP1-2.6, SSP2-4.5, SSP3-7.0, and SSP5-8.5.

TABLE II. CMIP6 MODEL DETAILS

Model	Modeling Centre	Resolution (longitude × latitude)
BCC	Beijing Climate Centre, China	320 × 160, L46 (T106)
Can	Canadian Centre for Climate Modeling and Analysis, Canada	128 × 64, L49 (T63)

III. METHODOLOGY

A. Data Interpolation

Linear interpolation is performed to data from [18] to estimate the values at the selected station locations. This numerical technique is applied to estimate the unknown values within a range of known data points and is computationally efficient, preserving the trend of the original data without introducing significant distortions. Given two known points (x_1, y_1) and (x_2, y_2), the interpolated value y at a given x is computed using:

$$y = y_1 + \frac{(y_2 - y_1)}{(x_2 - x_1)}(x - x_1) \quad (1)$$

B. Statistical Deterministic Metrics

The climatological mean is used to assess how effectively the CMIP6 modeling captures the yearly cycles and patterns of inter-annual variability. The performance of CMIP6 simulations is examined through five continuous statistical measures and four categorical indices calculated throughout the three rain gauge sites in the Subarnarekha River basin. To visualize the geographic patterns in comparison to the observable reference datasets, ArcGIS 10.4 and the R statistical package are utilized. The continuous indices are presented below with the first being CC. This index refers to the degree of correlation between each of the two distinct models and the observed source datasets. The CC ideal value is 1.0 and is calculated by:

$$\mathrm{CC} = \frac{\sum(O-\bar{O})(P-\bar{P})}{\sqrt{\sum(O-\bar{O})^2 \sum(P-\bar{P})^2}} \quad (2)$$

where $\overline{O}$ and $\overline{P}$ represent the mean of the observed (O) and predicted (P) data respectively. The Percent Bias ratio (PBIAS) evaluates whether the model's simulation values are higher or lower than the observed values. A perfect PBIAS score is 0.0, with low-magnitude values indicating accurate model simulations. Positive PBIAS values suggest that the model overestimates the observed values, while negative values indicate their underestimation. PBIAS is employed to assess the variability among the two CMIP6 models in their simulation of the observed rainfall amounts and is computed by:

$$\mathrm{PBIAS} = \frac{\sum(P-O)}{\sum(O)} \times 100 \quad (3)$$

RMSE measures the average magnitude of the error between the predicted and observed values in a dataset. It is calculated as the square root of the average of the squared differences between the predicted and observed values, providing a sense of how close the model's predictions are to the actual data. RMSE values close to zero indicate better model performance and are calculated by:

$$\mathrm{RMSE} = \sqrt{\frac{\sum(P-O)^2}{N}} \quad (4)$$

where N is the total number of data points. The Nash– Sutcliffe Efficiency (NSE) metric is calculated using:

$$\mathrm{NSE} = 1 - \frac{\sum(P-O)^2}{\sum(O-\bar{O})^2} \quad (5)$$

The categorical indices are employed to assess the performance of the satellite products taking into account the occurrence and non-occurrence of the rainfall events. To begin with, the Probability of Detection (POD) is a statistical measure used to evaluate the performance of binary classification systems, particularly in scenarios where detecting the occurrence of an event is critical. In the context of rainfall prediction, POD measures the proportion of the observed rainfall events that are correctly predicted by the model as rainfall. POD ranges from 0 to 1, with values closer to 1 indicating the model's superior ability in forecasting the precipitation occurrences:

$$\mathrm{POD} = \frac{\mathrm{TP}}{\mathrm{TP+FN}} \quad (6)$$

The number of successfully predicted and incorrectly predicted rainfall occurrences is represented by True Positives (TP) and False Negatives (FN), respectively. False Positives (FP) refer to the incorrect predictions of an event when it has not occurred, while TP to the successful predictions when the event has occurred.

Furthermore, Probability of False Detection (POFD) is a metric used to evaluate the performance of a binary classification system. The range of the POFD typically lies between 0 and 1. A POFD value of 0 indicates that there are no false detections, and 1 indicates that all the predicted events when no event is observed are false alarms:

$$\mathrm{POFD} = \frac{FP}{FP+TN} \quad (7)$$

Moreover, False Alarm Ratio (FAR) is a metric commonly utilized in the evaluation of binary classification systems, particularly in scenarios where the occurrence of an event is being predicted. FAR ranges from 0 to 1, with values closer to 0 indicating the model's superior capacity to record the precipitation occurrences:

$$\mathrm{FAR} = \frac{FP}{FP+TP} \quad (8)$$

Finally, the ratio of precipitation occurrences that the model has accurately identified is represented by the Critical Success Index (CSI). This indicator has a value between 0 and 1, with the model performance being optimal when its value is near to 1:

$$\mathrm{CSI} = \frac{TP}{TP+FP+FN} \quad (9)$$

C. Trend Detection

The MK test is a non-parametric method to detect statistically significant trends in time-series. The data are evaluated in a time-ordered sequence, with each value being compared to all subsequent values. Let n data points be represented by $x_1, x_2, \ldots, x_n$, and the MK statistics (S) is defined by:

$$S = \sum_{k=1}^{n-1} \sum_{j=k+1}^{n} sign(x_j - x_k) \quad (10)$$

where x_j and x_k are two generic data values in sequence The function $sign(x_j - x_k)$ takes the values indicated by:

$$sign(x_j - x_k) = \begin{cases} 1, & if\ (x_j - x_k) > 0, \\ 0, & if\ (x_j - x_k) = 0, \\ -1, & if\ (x_j - x_k) < 0. \end{cases} \quad (11)$$

A positive S value indicates an increasing trend, while a negative one indicates a decreasing trend. The S statistic represents the difference between the number of positive and negative differences in the under-study time-series. Under the null hypothesis, the statistic S follows a normal distribution with the mean $E(S)$ and variance Var(S), as described by:

$$E(S) = 0 \quad (12)$$

$$Var(S) = \frac{1}{18}[n(n-1)(2n+5) - \sum_{p-1}^{q} t_p(t_p-1)(2t_p+5)] \quad (13)$$

where q is the total number of the tied values, t_p is the number of ties for the p^{th} value, and n is the length of the time-series. Adjustments for tied or censored data are considered in the second term. Equation (14) is the definition of the standardized test statistic Z:

$$Z = \begin{cases} \frac{S-1}{\sqrt{Var(S)}}, & if\ S > 0, \\ 0, & if\ S = 0, \\ \frac{S+1}{\sqrt{Var(S)}}, & if\ S < 0. \end{cases} \quad (14)$$

The Z value is used to assess the presence of a statistically significant trend by testing the null hypothesis that no trend exists. A positive Z indicates an increasing trend, while a negative Z indicates a decreasing trend. At a specific significance level, the null hypothesis is rejected if the absolute Z value exceeds $Z(1-p/2)$, derived from standard normal distribution tables. In this study, a 0.05 significance level is selected. A p-value less than 0.05 indicates a statistically significant trend, while a p-value greater than 0.05 suggests no significant trend.

D. Sen's Slope Estimator

The magnitude of a trend in a time-series is estimated using Sen's Slope estimator, a non-parametric approach that calculates the slope (T_i) of all data pairs under the assumption of a linear trend and is calculated by:

$$T_i = \frac{X_j - X_k}{j-k} \quad (15)$$

where $i = 1, 2, \ldots, n$, X_j and X_k are the data values at timestep/timesteps j and k, with $j > k$, respectively. The median of these T_i values provides the Sen's slope estimator (β). A positive β signifies an increasing trend, while a negative β a decreasing [19].

IV. RESULTS AND DISCUSSION

A. Descriptive Statistics of CMIP6 Against Observed Data

Table III presents the descriptive statistics between CMIP6 and the observed data. The findings demonstrate that the SSP3-7.0 of BCC model shows the most optimal result regarding the PBIAS value in the Upper region. The minimum PBIAS value is observed in the Middle region for the SSP2-4.5 scenario of the BCC model. In the Lower region regarding SSP2-4.5, the BCC model presents a more accurate match in post monsoon season, also reflected by the lower PBIAS value. However, the SSP5-8.5 scenario of BCC aligns with the annual rainfall in-spite-of having a higher PBIAS value. This correlation is also confirmed by the statistical value of CC of SSP5-8.5 of the BCC model.

The results from the performance analysis of categorical indices are presented in Table IV. The following scenarios of the BCC model: SSP3-7.0 in the Upper region, SSP2-4.5 in the Middle region, and SSP2-4.5 and SSP5-8.5 in the Lower region suggest better POFD and CSI values with the observed data. The BCC model demonstrates superior performance in terms of the POD and FAR values when compared to the Can model.

TABLE III. CONTINUOUS INDEX PERFORMANCE EVALUATION OF GCMS

Region	Model	Scenarios	CC	PBIAS	RMSE	NSE
Upper	BCC	SSP1-2.6	0.21	16.79	40.52	-0.30
		SSP2-4.5	0.25	15.24	39.28	-0.22
		SSP3-7.0	0.23	11.88	40.18	-0.28
		SSP5-8.5	0.17	23.82	40.49	-0.30
	Can	SSP1-2.6	0.30	44.13	37.85	-0.14
		SSP2-4.5	0.27	40.96	38.33	-0.16
		SSP3-7.0	0.20	28.55	42.31	-0.42
		SSP5-8.5	0.18	31.90	40.85	-0.32
Middle	BCC	SSP1-2.6	0.31	32.38	54.79	0.00
		SSP2-4.5	0.19	16.86	60.42	-0.21
		SSP3-7.0	0.19	21.99	61.75	-0.27
		SSP5-8.5	0.12	30.25	62.57	-0.30
	Can	SSP1-2.6	0.38	48.80	54.66	0.01
		SSP2-4.5	0.26	49.38	57.52	-0.10
		SSP3-7.0	0.32	40.60	56.83	-0.07
		SSP5-8.5	0.13	34.16	64.15	-0.37
Lower	BCC	SSP1-2.6	0.40	19.28	43.98	0.06
		SSP2-4.5	0.41	13.12	45.26	0.00
		SSP3-7.0	0.02	22.00	55.87	-0.52
		SSP5-8.5	0.41	21.89	44.44	0.04
	Can	SSP1-2.6	0.23	33.36	53.60	-0.40
		SSP2-4.5	0.47	43.55	44.36	0.04
		SSP3-7.0	0.35	42.06	49.01	-0.17
		SSP5-8.5	0.18	15.12	66.00	-1.12

TABLE IV. CATEGORICAL INDEX PERFORMANCE EVALUATION OF GCMS

Region	Model	Scenarios	POD	POFD	FAR	CSI
Upper	BCC	SSP1-2.6	0.92	0.89	0.13	0.81
		SSP2-4.5	0.98	1.00	0.12	0.87
		SSP3-7.0	0.96	1.00	0.12	0.88
		SSP5-8.5	0.92	1.00	0.14	0.80
	Can	SSP1-2.6	0.90	0.89	0.13	0.80
		SSP2-4.5	0.95	0.67	0.09	0.87
		SSP3-7.0	0.90	1.00	0.14	0.79
		SSP5-8.5	0.90	1.00	0.14	0.79
Middle	BCC	SSP1-2.6	0.90	1.00	0.17	0.76
		SSP2-4.5	0.97	1.00	0.13	0.84
		SSP3-7.0	0.98	0.91	0.16	0.83
		SSP5-8.5	0.90	1.00	0.17	0.76
	Can	SSP1-2.6	0.92	0.82	0.15	0.79
		SSP2-4.5	0.97	0.73	0.11	0.87
		SSP3-7.0	0.92	0.91	0.14	0.80
		SSP5-8.5	0.87	1.00	0.17	0.73
Lower	BCC	SSP1-2.6	0.92	1.00	0.11	0.83
		SSP2-4.5	0.94	1.00	0.10	0.84
		SSP3-7.0	0.94	1.00	0.11	0.86
		SSP5-8.5	0.95	1.00	0.12	0.85
	Can	SSP1-2.6	0.91	0.86	0.09	0.83
		SSP2-4.5	0.91	0.86	0.11	0.82
		SSP3-7.0	0.92	0.86	0.09	0.84
		SSP5-8.5	0.86	1.00	0.10	0.79

Furthermore, the Taylor diagrams are illustrated in Figure 2 for the statistical comparison of the standard deviation and CC in all three regions. The BCC model presented higher values of CC with the observed rainfall data with a slight reduction in the standard deviation in Upper and Lower regions. However the

CC in middle region exhibited a slightly higher standard deviation from the reference line than the other two regions. The Can model suggests similar standard deviation values with the reference data and presented the opposite behavior in terms of CC. Overall the models offered an average CC of 0.4 with an average standard deviation between 30% and 40% in all three regions.

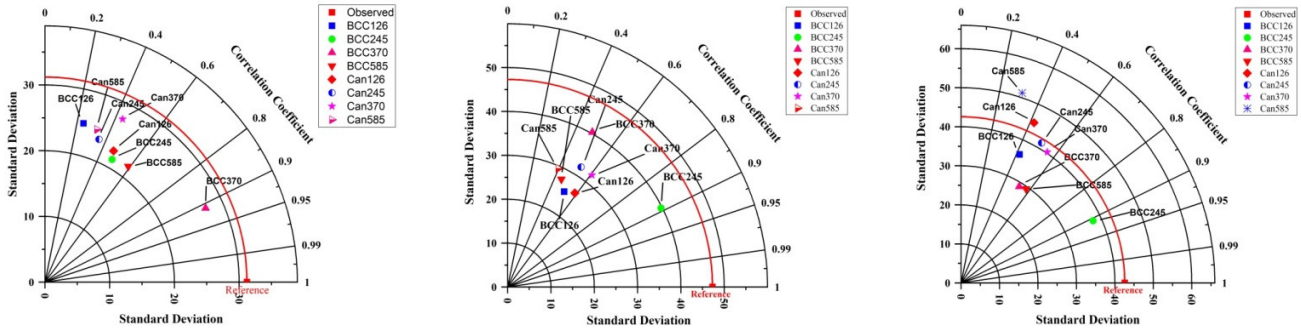

Fig. 2. Taylor diagrams comparing simulated rainfall from BCC and Can models with observed data at: (a) Upper (Ranchi), (b) Middle (Jamshedpur), and (c) Lower (Digha) regions. The subsequent numbers after the model abbreviation (i.e., 126, 245, 370, and 585) are the representation of different scenarios (i.e., SSP1-2.6, SSP2-4.5, SSP3-7.0, and SSP5-8.5) under each model.

TABLE V. TREND ANALYSIS OF MONTHLY OBSERVED AND SIMULATED RAINFALL DATA

Month	Statistic	Upper		Middle		Lower		
		Observed	SSP3-7.0	Observed	SSP2-4.5	Observed	SSP2-4.5	SSP5-8.5
January	*p*	0.47	0.35	0.69	0.18	0.57	0.93	0.42
	Z	-0.72	-0.94	-0.40	1.34	-0.57	-0.09	-0.81
	Slope	-0.13	-0.05	0.00	0.07	0.00	0.00	0.00
February	*p*	0.12	0.37	0.72	0.65	0.44	0.88	0.90
	Z	-1.57	-0.90	-0.36	0.45	-0.78	0.15	0.12
	Slope	-0.39	-0.04	-0.01	0.02	-0.01	0.00	0.00
March	*p*	0.66	0.75	0.52	0.16	0.63	0.84	0.32
	Z	-0.44	0.32	-0.64	-1.39	-0.47	0.20	1.00
	Slope	-0.12	0.02	-0.21	-0.06	-0.12	0.00	0.03
April	*p*	0.88	0.83	0.95	0.38	0.34	0.95	0.23
	Z	-0.15	0.21	-0.06	-0.88	-0.95	0.06	1.20
	Slope	-0.08	0.01	0.00	-0.02	-0.46	0.00	0.02
May	*p*	0.88	0.81	0.79	0.20	0.52	0.21	0.59
	Z	-0.15	-0.25	-0.27	1.27	-0.64	1.26	0.54
	Slope	-0.08	-0.01	-0.25	0.05	-1.08	0.01	0.01
June	*p*	0.00	0.03	0.00	0.02	0.02	0.04	0.23
	Z	-2.91	-1.04	-3.29	-0.20	-2.30	1.73	1.20
	Slope	-6.95	0.08	-8.13	-0.01	-5.41	0.03	0.02
July	*p*	0.61	0.22	0.39	0.11	0.09	0.26	0.63
	Z	-0.50	1.23	-0.86	1.60	-1.69	1.12	-0.48
	Slope	-1.29	0.10	-3.31	0.15	-3.99	0.07	-0.06
August	*p*	0.07	0.74	0.61	0.01	0.22	0.05	0.24
	Z	-1.81	0.34	-0.50	2.45	-1.22	1.93	1.18
	Slope	-4.79	0.03	-1.78	0.18	-3.86	0.24	0.16
September	*p*	0.07	0.54	0.25	0.65	0.30	0.35	0.00
	Z	-1.79	0.61	-1.16	-0.45	-1.04	-0.94	2.87
	Slope	-4.17	0.06	-3.43	-0.05	-3.66	-0.13	0.39
October	*p*	0.94	0.61	0.70	0.12	0.44	0.09	0.06
	Z	-0.07	-0.51	-0.39	1.56	-0.77	1.72	1.90
	Slope	-0.12	-0.03	-0.37	0.14	-2.28	0.24	0.33
November	*p*	0.28	0.21	0.22	0.59	0.11	0.18	0.07
	Z	-1.08	-1.26	-1.23	0.54	-1.61	1.34	1.78
	Slope	-0.01	-0.05	-0.02	0.02	-0.83	0.09	0.19
December	*p*	0.25	0.32	0.46	0.21	0.10	0.23	0.84
	Z	-1.16	1.00	0.74	-1.25	1.66	1.20	0.20
	Slope	-0.86	0.06	0.00	-0.06	0.00	0.02	0.00

B. Trend Analysis

The trend analysis of the monthly observed and simulated rainfall data is performed in all three regions utilizing the MK test and Sen's slope estimator to identify the trends over the past years. The results are presented in Table V. In the analysis, the following scenarios are considered: SSP3-7.0 in the Upper region, SSP2-4.5 in the Middle region, and SSP2-4.5 and SSP5-8.5 in the Lower region, as they yielded the most optimal results. For the Upper region in June, the p-value is 0.00 regarding the observed data, whereas for the SSP3-7.0 scenario is 0.03 with both exhibiting a negative trend. For the same month in the Middle region the p-values are 0.00 and 0.02 for the observed and SSP2-4.5 data, respectively, with also both highlighting a negative trend. In the Lower region, in June, the p-values are 0.02, 0.04, and 0.23 for the observed, SSP2-4.5, and SSP5-8.5 with a negative trend for the observed and a positive trend for the other two. Overall, most months and regions suggest negative trends, especially during summer, indicating decreasing values over time. However, the SSP2-4.5 and SSP5-8.5 scenarios tend to show small or neutral zero trends, suggesting a potential stabilization or reversal of the past declines depending on the scenario and region

V. CONCLUSIONS

Monthly rainfall data from 2015 to 2023 were analyzed alongside simulated rainfall data from CMIP6 models across three different regions. The study aimed to determine the CMIP6 model that most accurately represents the observed rainfall patterns in the Subarnarekha River basin situated in Eastern India. For this purpose, continuous and categorical indices were calculated across different Shared Socioeconomic Pathways (SSP) scenarios. Among the tested models, BCC-CSM2-MR (BCC) consistently demonstrated superior performance in all regions during the monsoon season against CanESM5 (Can), which suggested poor accuracy in the rainfall prediction. The results were validated through Taylor diagrams, which yielded similar results. Furthermore, the analysis revealed that the models achieved an average Correlation Coefficient (CC) of 0.4, with standard deviations ranging between 30% and 40% when compared to the observed data.

Finally, the trends in both the observed and simulated rainfall data under the best-performing scenarios were assessed using the Mann–Kendall (MK) trend test and Sen's slope estimator. The results highlighted a not statistically significant negative trend in most cases, except for June, where statistically significant positive trends were dominant.

ACKNOWLEDGMENT

The authors would like to thank the India Meteorological Department for providing daily rainfall data (2015-2023) and online sources, namely Bias-corrected daily projections of precipitation from CMIP6 [18], website [20] for providing daily precipitation data (2015-2023), that are used for carrying out this research work.

REFERENCES

[1] Intergovernmental Panel on Climate Change (IPCC), *AR5 Climate Change 2014: Impacts, Adaptation, and Vulnerability*. Cambridge, UK: Cambridge University Press, 2014.

[2] C. C. Maxino, B. J. McAvaney, A. J. Pitman, and S. E. Perkins, "Ranking the AR4 climate models over the Murray-Darling Basin using simulated maximum temperature, minimum temperature and precipitation," *International Journal of Climatology*, vol. 28, no. 8, pp. 1097–1112, Aug. 2008, https://doi.org/10.1002/joc.1612.

[3] S. Kumar and V. Singh, "Variation of extreme values of rainfall and temperature in Subarnarekha River basin in India," *Journal of Water and Climate Change*, vol. 15, no. 3, pp. 921–939, Feb. 2024, https://doi.org/10.2166/wcc.2024.364.

[4] E. Hawkins and R. Sutton, "The potential to narrow uncertainty in projections of regional precipitation change," *Climate Dynamics*, vol. 37, no. 1, pp. 407–418, Apr. 2010, https://doi.org/10.1007/s00382-010-0810-6.

[5] L. Agel, M. Barlow, J. Polonia, and D. Coe, "Simulation of Northeast U.S. Extreme Precipitation and Its Associated Circulation by CMIP5 Models," *American Meteorological Society*, vol. 33, pp. 9817–9834, Oct. 2020, https://doi.org/10.1175/JCLI-D-19- 0757.s1.

[6] D. Vinod and V. Agilan, "Ranking of CMIP 6 climate models in simulating precipitation over India," *Acta Geophysica*, vol. 72, no. 5, pp. 3703–3717, 20204-03-08, https://doi.org/10.1007/s11600-024-01313-7.

[7] S. Shetty, P. Umesh, and A. Shetty, "Future transition in climate extremes over Western Ghats of India based on CMIP6 models," *Environmental Monitoring and Assessment*, vol. 195, no. 5, Apr. 2023, Art. no. 578, https://doi.org/10.1007/s10661-023-11090-3.

[8] V. Eyring *et al.*, "Overview of the Coupled Model Intercomparison Project Phase 6 (CMIP6) experimental design and organization," *Geoscientific Model Development*, vol. 9, no. 5, pp. 1937–1958, May 2016, https://doi.org/10.5194/gmd-9-1937-2016.

[9] S. Ranjan and V. Singh, "ANN and GRNN-Based Coupled Model for Flood Inundation Mapping of the Punpun River Basin," *Engineering, Technology & Applied Science Research*, vol. 13, no. 1, pp. 9941–9946, Feb. 2023, https://doi.org/10.48084/etasr.5483.

[10] D. Maraun *et al.*, "Precipitation downscaling under climate change: Recent developments to bridge the gap between dynamical models and the end user," *Reviews of Geophysics*, vol. 48, no. 3, Sept. 2010, https://doi.org/10.1029/2009RG000314.

[11] K. Praveen and L. B. Roy, "Assessment of Groundwater Quality Using Water Quality Indices: A Case Study of Paliganj Distributary, Bihar, India," *Engineering, Technology & Applied Science Research*, vol. 12, no. 1, pp. 8199–8203, Feb. 2022, https://doi.org/10.48084/etasr.4696.

[12] S. Ranjan and V. Singh, "Effect of land use land cover changes on hydrological response of Punpun River basin," *Environmental Monitoring and Assessment*, vol. 195, no. 9, Sept. 2023, Art. no. 1137, https://doi.org/10.1007/s10661-023-11785-7.

[13] V. Mishra, U. Bhatia, and A. D. Tiwari, "Bias-corrected climate projections for South Asia from Coupled Model Intercomparison Project-6," *Scientific Data*, vol. 7, no. 1, Oct. 2020, Art. no. 338, https://doi.org/10.1038/s41597-020-00681-1.

[14] A. Towheed and R. Thendiyath, "Spatiotemporal Rainfall Dynamics in Kosi Basin Using Wavelet Analysis," *Engineering, Technology & Applied Science Research*, vol. 11, no. 5, pp. 7578–7584, Oct. 2021, https://doi.org/10.48084/etasr.4372.

[15] A. K. Singh and S. Giri, "Subarnarekha River: The Gold Streak of India," in *The Indian Rivers: Scientific and Socio-economic Aspects*, D. S. Singh, Ed. Singapore, Singapore: Springer, 2018, pp. 273–285.

[16] U. Mandal, D. R. Sena, A. Dhar, S. N. Panda, P. P. Adhikary, and P. K. Mishra, "Assessment of climate change and its impact on hydrological regimes and biomass yield of a tropical river basin," *Ecological Indicators*, vol. 126, July 2021, Art. no. 107646, https://doi.org/10.1016/j.ecolind.2021.107646.

[17] ESGF. "CMIP6 Search." Earth System Grid Federation. https://esgf-node.llnl.gov/search/cmip6/.

[18] D. M. Jose, A. M. Vincent, and G. S. Dwarakish, "Improving multiple model ensemble predictions of daily precipitation and temperature through machine learning techniques," *Scientific Reports*, vol. 12, no. 1, Mar. 2022, Art. no. 4678, https://doi.org/10.1038/s41598-022-08786-w.

[19] A. Mondal, D. Khare, and S. Kundu, "Spatial and temporal analysis of rainfall and temperature trend of India," *Theoretical and Applied*

Climatology, vol. 122, no. 1, pp. 143–158, Oct. 2014, https://doi.org/10.1007/s00704-014-1283-z.

[20] Mishra, Vimal; Bhatia, Udit; Tiwari, Amar Deep. "Bias corrected climate projections for South Asia from CMIP6 models." Zenodo. https://zenodo.org/record/3874046.